Journal of Hydrology: Regional Studies 10 (2017) 133–144

Contents lists available at ScienceDirect

Journal of Hydrology: Regional Studies

journal homepage: www.elsevier.com/locate/ejrh

Factors controlling the evolution of groundwater dynamics and chemistry in the Senegal River Delta

Abdoul Aziz Gning[a,b], Philippe Orban[a], Julie Gesels[a], Fatou Diop Ngom[b], Alain Dassargues[a], Raymond Malou[b], Serge Brouyère[a,*]

[a] Hydrogeology and Environmental Geology, Department ArGEnCo, Urban & Environmental Research Unit, University of Liège, Belgium
[b] Cheikh Anta Diop University in Dakar, Department of Geology, Hydrogeology Laboratory, Senegal

ARTICLE INFO

Article history:
Received 14 July 2015
Received in revised form 18 January 2017
Accepted 29 January 2017

Keywords:
Senegal River Delta
Groundwater–surface water interaction
Hydrogeochemistry
Saline water
Irrigation
Soil salinization

ABSTRACT

Study region: Senegal River Delta.
Study focus: The Senegal River Delta is a strategic region for the development of irrigated agriculture. Despite a Sahelian climatic context, the management of the river with dams ensures water availability throughout the year. With the intensification of agriculture, degradation of cultivated soils is observed, mostly linked to the existence of a shallow salty aquifer. In this context, regional surveys were performed to characterize groundwater–surface water interactions and to identify the impact of artificial river management and agricultural intensification on the evolution of groundwater dynamics and chemistry.
New hydrological insights for the region: Results show that groundwater far away from rivers and outside irrigated plots has evolved from marine water to brines under the influence of evapotranspiration. Near rivers, salinity of groundwater is lower than seawater and groundwater mineralization seems to evolve in the direction of softening through cationic exchanges related to permanent contact with fresh water. Despite large volumes of water used for rice cultivation, groundwater does not show any real softening trend in the cultivated parcels. Results show that the mechanisms that contribute to repel salt water from the sediments correspond to a lateral flush near permanent surface water streams and not to vertical drainage and dilution with rainfall or irrigation water. It is however difficult to estimate the time required to come back to more favorable conditions of groundwater salinity.

1. Introduction

The Senegal River Delta (SRD) has a great potential of agricultural land, estimated at 150,000 ha and a large availability of water through the Senegal River. It is for this purpose an agro-economic zone of major importance for the development of irrigated agriculture and food self-sufficiency in Senegal. However, the practice of irrigated agriculture in the SRD is now seriously threatened by salinization leading to the abandonment of many developed areas (Barbiéro and Laperrousaz, 1999).

* Corresponding author at: University of Liège, Hydrogeology and Environmental Geology, Department ArGEnCo, Urban & Environmental Engineering Research Unit, Building B52/3, 4000 Sart Tilman, Liège, Belgium.
E-mail addresses: gningabdoul@gmail.com (A.A. Gning), Serge.Brouyere@ulg.ac.be (S. Brouyère).

http://dx.doi.org/10.1016/j.ejrh.2017.01.005

Most studies on this salinization question have pointed the presence of a shallow (maximum 2 m depth) salty aquifer resulting from alternating episodes of marine transgressions and regressions that have driven the evolution of the SRD during the Quaternary (Audibert, 1970; Trénous and Michel, 1971; Michel, 1973; Loyer, 1989; Ceuppens et al., 1997; Barbiéro et al., 2004). In addition, in a recent past, sea waters continued to frequently invade the floodplains of the river during low surface water levels (Cogels, 1994; Gac et al., 1986). To face these invasions, the countries bordering the river, associated within the OMVS interstate organization (Senegal River Basin Development Authority), built the anti-salt Diama dam in 1986 (26 km upstream of St. Louis). A second dam was erected in 1988 at Manantali in the Malian territory to store the surplus rainwater on the upper basin. It took more or less 10 years to reach equilibrium of river water levels at 1.5 m above sea level upgradient from the Diama dam (Gning, 2015). From that time, the combined management of both dams has helped maintaining sufficient water for irrigation of agricultural areas throughout the year and the emergence and diversification of agricultural production systems. Many programs have been developed in the SRD with the primary objective of achieving food self-sufficiency, resulting in an intensification of agricultural activities, an increase in planted areas and in volumes of water used for irrigation.

However, this improvement in water availability and increased irrigation have certainly had hydrological and hydrochemical consequences, particularly on the shallow aquifer. In this context, the objective of the research is to establish a conceptual model describing the origin and evolution of groundwater chemistry in the SRD, and the impact, at regional scale, of the artificial river management and agricultural intensification on this evolution, as a support for future solutions of water management for sustainable agriculture in this region.

2. Description of the study area

The SRD is located northwest of Senegal, 260 km from the capital Dakar. On the Senegalese side, it covers an area of 3500 km^2, extending over a length of 250 km from Richard Toll to St Louis (Fig. 1). This area is dominated by vast flatlands limited to the north by the Senegal River, to the west by the Atlantic Ocean, to the east by the Guiers Lake, to south-west by dunes and southeast by the Ferlo Valley (not shown in Fig. 1).

In this North Sahelian zone, annual rainfall does not go beyond 400 mm/year and potential evapotranspiration reaches 2500 mm/year (Diaw, 1996; Malou, 2004; Diaw, 2008). The hydrographic network is very dense and includes the main branch of the river Senegal which has many distributaries. The river also feeds, through the Taoué channel, the Guiers Lake which is a depression of 300 km^2 (Fall, 2006). The various distributaries of the river and the lake allow irrigation of many agricultural areas (light green patterns in Fig. 1) by a complex system of watercourses and open channels. Rice, which is the main crop in the delta, is irrigated by submersion, maintaining a significant layer of water on the soil surface for several

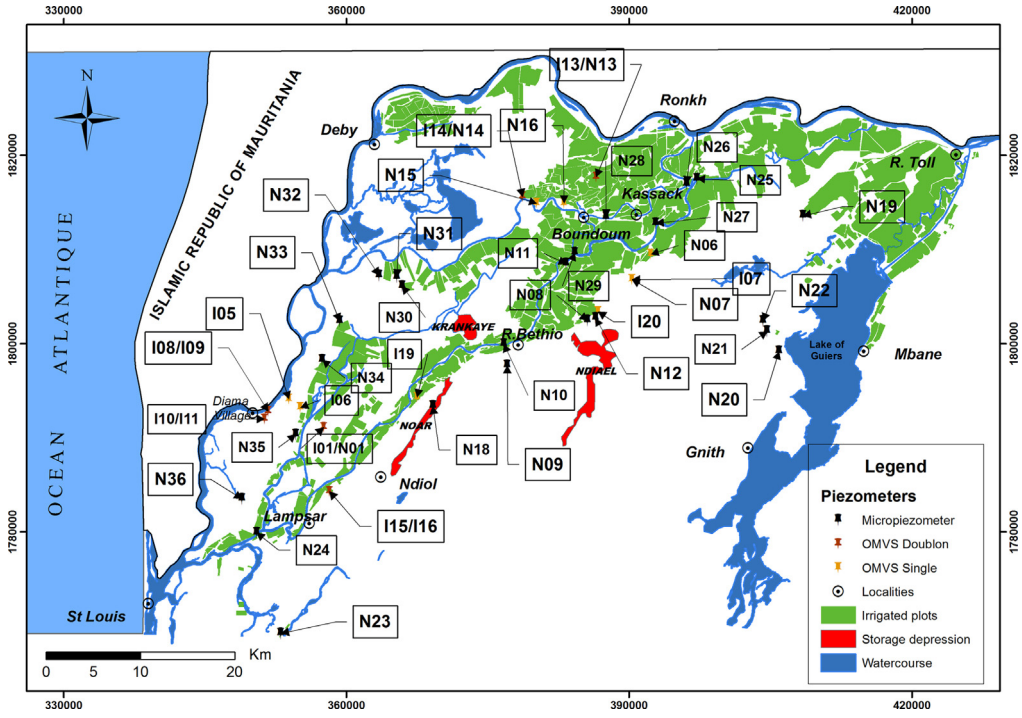

Fig. 1. Location map and main features of the Senegal River Delta. (For interpretation of the references to color in the text, the reader is referred to the web version of this article.)

months (Gning et al., 2012). Drainage water from these areas is evacuated via channels and discharged into the Ndiael, Noar and Krankaye natural depressions (red patterns in Fig. 1).

The geological formations are dominated by alluvial deposits of Quaternary age, set up during alternating periods of marine transgressions and regressions. The most important were deposited during the Inchirian (40,000–31,000 years BP) and Nouakchottian (around 5500 years BP) periods (Roger et al., 2009; Sarr et al., 2008). From place to place, the Nouakchottian may be absent.

From a hydrogeological point of view, several aquifers are present, including the superficial alluvial aquifer investigated in this study. This aquifer is made of two reservoirs (PGE, 1998). The first (upper) reservoir is located in fine to clayey sands of Nouakchottian age. It has a mean thickness of 11 m and it is overlaid from place to place by a semi-permeable clayey to silty recent deposits, which induce locally semi-confined conditions. The second (lower) reservoir is located in fine to coarse sands of Inchirian age. It is also overlain by a semi-permeable layer of silt and clay that forms the top of the Inchirian. This semi-permeable layer is discontinuous, which allows locally a hydraulic continuity between the two compartments (OMVS/USAID, 1990).

3. Research methodology

3.1. Groundwater and surface water monitoring network

To meet the objectives of the study, the methodological approach is based on the monitoring of the dynamics of the groundwater table coupled to hydrogeochemical surveys. The groundwater monitoring network is made of 46 access points (see Table S1 in Supplementary Material 1 for further details). 21 piezometers drilled by OMVS after impoundment of the dams were identified in the field and rehabilitated in the scope of our project. Among these, 12 are collocated and screened at two different depths. In addition, 24 shallow micropiezometers (max. 6 m) were drilled with a hand auger in the scope of our project. Finally, one traditional well was identified in the village of Diama. For practical reasons, all these piezometers were renamed according to the reservoir in which they are screened: Ixx and Nxx for those screened in the Inchirian and Nouakchottian reservoirs respectively.

On this network, measurements of groundwater levels were conducted monthly between April 2011 and January 2014. Historical data on piezometric levels, collected between 1997 and 2002 (PGE, 1998) were also considered for comparison with current measurements. All these piezometric data were compared with monthly rainfall measured at the St Louis station and with river water levels monitored at the Diama dam upstream station.

For the hydrogeochemical study, two sampling campaigns were organized, the first at the end of the dry season (June 2012), the second after the rainy season (October 2012). Groundwater samples were collected in the two groundwater reservoirs: in 12 OMVS piezometers, 17 micropiezometers and in the Diama traditional well (see Table S1 in SM 1). Samples were also taken in surface water (ES) feeding the irrigated parcels, in drainage water (ED) leaving these parcels, and in seawater (EM) and rainwater (EP).

3.2. Interpretation of regional scale groundwater chemistry

Chemical analyses obtained from the sampling campaigns were used to characterize the hydrochemistry of the aquifer. The comparative analysis of the two campaigns does not show any significant changes in water chemistry between the dry and rainy seasons. Considering this, the analysis and interpretation will subsequently be focused on the dry season survey, which involved more (35) sampling points.

3.2.1. Multivariate statistical analysis of hydrogeochemical data based on Self Organizing Maps

Statistical methods of multivariate analysis are increasingly used in the study of geochemical processes in natural waters (Belkhiri, 2011; Güler et al., 2002; Madioune, 2012; Mudry, 1991). They allow highlighting the relationships between parameters in the hydrogeological system where the evolution of the chemical composition of water is complex and depends on several processes that can influence each other.

A non-linear multivariate statistical technique is applied to investigate the dataset, the Kohonen's Self-Organizing Map (SOM) (Kohonen, 2001). The SOM is an artificial neural network algorithm based on unsupervised learning. The technique allows visualizing relations between parameters and separating the data set into different groups of similar chemical composition (Peeters et al., 2007). In the studied area, links will be sought between the spatial location of the groups, correlations between parameters and geochemical processes. The SOM allows to find complex non-linear relationships (Kohonen, 2001). Despite the transformations applied to the data when using PCA and FA, a non-linear technique such as SOMs outperforms linear techniques with hydrogeochemical data (Hong and Rosen, 2001; Gamble and Babbar-Sebens, 2012).

The final result produced by the SOM algorithm is a 2-dimensional matrix, m x n. The matrix generally contains more nodes ($m \times n$) than the number of samples. Each sample is associated to the node with the most similar chemical composition. Samples positioned close to each other in the matrix present generally the same type of chemical composition. Samples whose chemical composition is very close can be positioned on the same node. The resulting matrix is displayed using 2 images: the unified distance matrix (*U*-matrix) and the component planes (Vesanto et al., 1999).

The *U*-matrix shows the distance between each node and its neighbors (similar to very different composition). From this *U*-matrix, groups can be detected automatically using the SOM algorithm (Ultsh and Herrmann, 2005). Similarly, this type of representation makes it easy to identify a sample of unusual composition, which is considered a multivariate outlier.

The component planes represent the concentrations of each variable on the 2-dimensional matrix (Ultsh and Herrmann, 2005). The number of component planes is the same as the number of variables. Concentrations are represented by a range of colors. In our case, the nodes in blue are associated with the lowest concentrations and nodes in red are associated with the higher concentrations. Component planes comparison is used to find correlations between variables, based on the similarity of patterns obtained in the resulting rectangles. Correlated parameters show high concentrations (red) in the same areas of the matrix and low concentrations (blue) also in the same areas of the matrix. The chemical characteristics of each group are derived from component planes, visualizing the position of each group in the *U*-matrix and concentrations in the same area of the matrix for each component plane.

3.2.2. Determination of groundwater chemistry acquisition and evolution

Understanding the chemistry of groundwater in the SRD, characterized by very high salinity values, requires identifying the origin of salinity and the factors that control its evolution with time. Here, it is of course expected that sea water is the main source of salinity but interactions with subsurface deposits (e.g. mineral–water interactions, cationic exchange processes) and the interactions with surface water can also have, from place to place, a significant influence on the chemical composition of groundwater. Different methods are available in the literature to investigate factors controlling the chemical composition of natural waters. Those used in the present study are briefly described here.

The origin of groundwater salinity can be established using the Na/Cl binary diagram (Abid et al., 2011; Bourhane, 2010; Magaritz et al., 1981). A Na/Cl ratio of 1 indicates that salinity preferentially comes from the dissolution of halite (NaCl mineral). A Na/Cl ratio higher than 1 indicates enrichment in Na due to cation exchanges with clays or dissolution of silicate minerals (Awni, 2008). A Na/Cl ratio equal or close to 0.86 reflects a marine origin of water. Finally, a Na/Cl < 0.86 indicates that salinity is due to sea water that has evaporated and evolved to brines (Kloppmann et al., 2011).

Cation exchange processes can be identified in different ways. First, the Piper diagram (Piper, 1953) allows identifying the chemical facies of water samples based on the relative proportions of major anions and cations in their respective chemical compositions. However, through a facies comparison of different water samples, it further allows identifying the evolution of groundwater chemistry related to different factors such as mixing between different waters, cationic exchange related to "fresh" groundwater–sea water interactions, etc. (Appelo and Postma, 2005). Cationic exchange processes can be further demonstrated using the diagram which plots $(Ca + Mg) - (HCO_3 + SO_4)$ as a function of $(Na + K) - Cl$ (Abid et al., 2011; Garcia and Shigidi, 2006; Madioune, 2012) where the points should tend to align along a straight line of slope −1.

Secondary minerals are also likely to control the chemical composition of groundwater. The possible occurrence and influence of such secondary minerals can be determined by calculating their corresponding saturation indices (SI). Doing so requires geochemical modeling of water chemistry data, using advanced geochemical databases and tools (Deutsch, 1997). Here the calculation of mineral indices was performed using the well-known geochemical model PHREEQc (Parkhurst, 1995) with the help of the DIAGRAMMES software developed by the University of Avignon (Simler, 2009) and available at [http://www.lha.univ-avignon.fr/LHA-Logiciels.htm].

4. Results and discussion

4.1. Hydrodynamic behavior of the groundwater table

Comparison between groundwater levels at the 46 monitoring points to rainfall data and to surface water levels upstream the Diama dam shows that piezometers can be classified based on two main criteria (Table 1): (1) the distance to surface watercourses (influence of changes in surface water levels) and (2) the location within or outside agricultural areas (influence of irrigation). Group 1 includes piezometers located far from a surface watercourse (beyond 1000 m from the river) and outside any irrigated area. Group 2 includes piezometers close to a surface watercourse (Senegal River and its distributaries) but outside any irrigated area. Group 3 includes piezometers located far from any surface watercourse but located in irrigated areas and finally Group 4 consists of piezometers, both close to a surface watercourse and located in irrigated areas. For the sake of clarity one piezometer is selected in each group to illustrate the general behavior of the group (Figs. 2–5).

Fig. 2 shows the evolution of piezometric level at Piezometer I01, representative of the general behavior of Group 1. During the period from April 2011 to January 2014, a groundwater rebound is consistently observed during the rainy season, with a delayed response to rainfall events. The same trend is also observed during the period 1997–2002. This shows that

Table 1
Classification of piezometers depending on the distance to streams and location in an agricultural area, the number of piezometers in each group is defined in brackets.

Groups	Away from river	Close to river
Outside irrigated plots	Group 1 (14)	Group 2 (13)
In irrigated plots	Group 3 (13)	Group 4 (7)

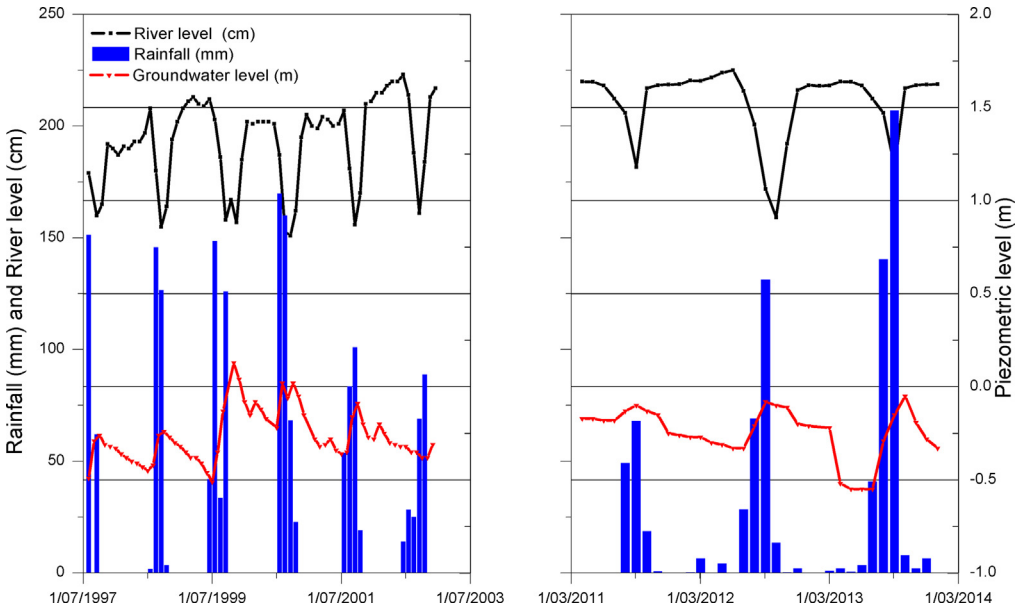

Fig. 2. Evolution of groundwater level at monitoring well I01 for the periods 1997–2001 and 2011–2014 and comparison with rainfall measured at the Saint-Louis station and surface water level measured at the Diama dam.

the groundwater table in this context is recharged by rain. During the dry season, the reverse process is observed, with a significant drop of the groundwater table explained by the important evaporation occurring during this season.

Fig. 3 shows the evolution of piezometric level at Piezometer I09 representative of the general behavior of Group 2. In this case, during the rainy season, when the river level drops in relation with water releases from the dam, a decline in the groundwater table is observed. On the contrary, during the dry season, the groundwater table rises in conjunction with the increase of water level in the river. The groundwater table response is also offset from the rising level of the river, showing the delay between surface and underground processes. Fluctuations in groundwater levels show a clear influence of changes in the Senegal River stage. In addition, the comparison of the two time periods 1997–2001 and 2011–2014 shows an increase of 1.5 m of the base level of the groundwater table, which has progressively equilibrated with the new reference level of surface water after the construction of the Diama dam.

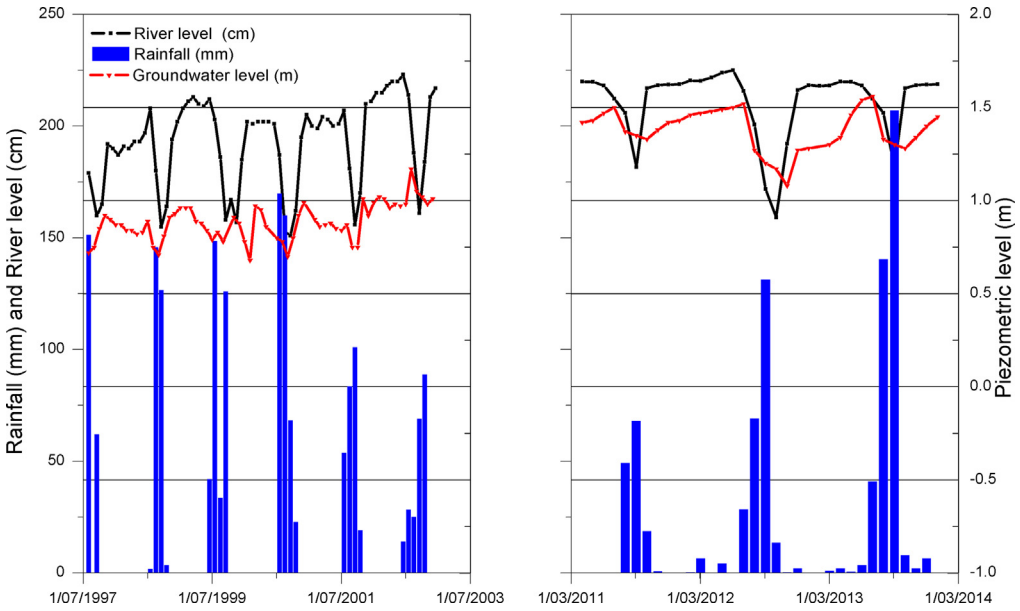

Fig. 3. Evolution of groundwater level at monitoring well I09 for the periods 1997–2001 and 2011–2014 and comparison with rainfall measured at the Saint-Louis station and surface water level measured at the Diama dam.

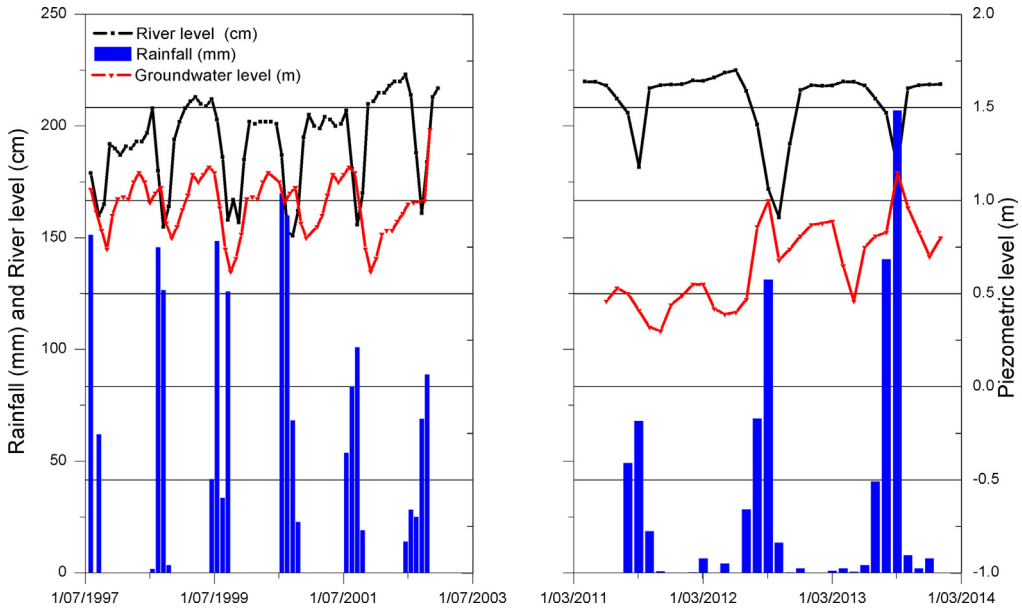

Fig. 4. Evolution of groundwater level at monitoring well I13 for the periods 1997–2001 and 2011–2014 and comparison with rainfall measured at the Saint-Louis station and surface water level measured at the Diama dam.

Fig. 4 shows the evolution of piezometric level at Piezometer I13 located 4000 m from the Senegal River, in the Boundoum irrigated area and representative of the general behavior of Group 3. During the most recent period of monitoring (2011–2014), fluctuations in groundwater levels allow identifying two periods corresponding to groundwater recharge events. The first period corresponds to natural recharge during the rainy season followed by a period of groundwater decline during the dry season. The second period corresponds to groundwater recharge related to irrigation practices. In the historical data (1997–2001), groundwater levels only react to rainfall events. From 2001 however, an additional period of rising groundwater level is observed during the dry season. This corresponds with the beginning of agricultural development in this sector of the Delta, more particularly to periods with submersed irrigated rice plots. In sectors corresponding to Group 3, groundwater is thus now recharged by rainfall during the rainy season but also by irrigation water during the dry season.

Fig. 5 shows the evolution of piezometric level at Piezometer I15 close to a river and located in an irrigated area, representative of Group 4. These piezometers are characterized by very irregular variations in groundwater levels reflecting the

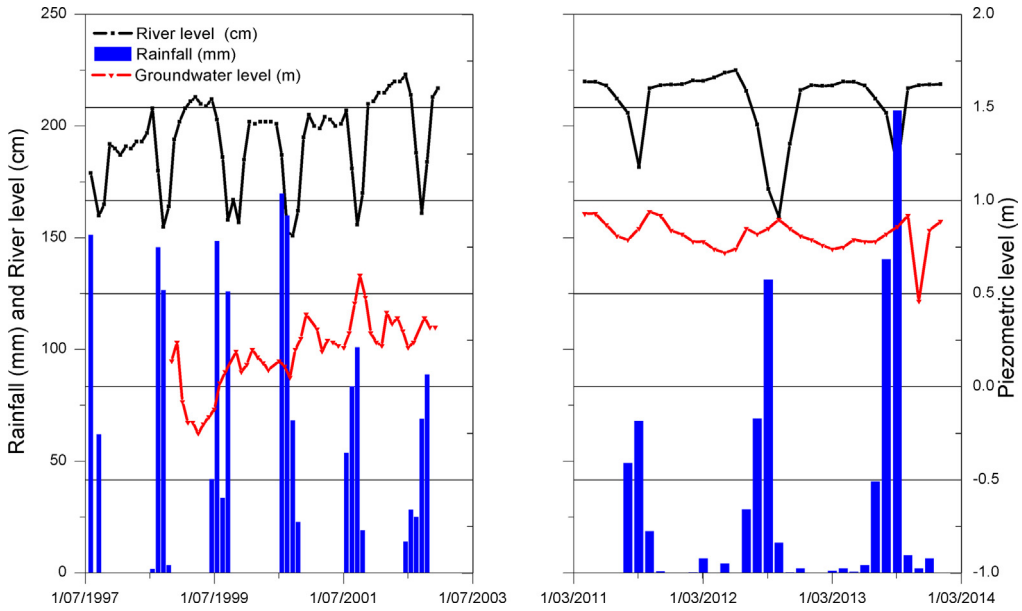

Fig. 5. Evolution of groundwater level at monitoring well I15 for the periods 1997–2001 and 2011–2014 and comparison with rainfall measured at the Saint-Louis station and surface water level measured at the Diama dam.

concomitant influence of changes in river stage and irrigation during the dry season. The influence of the construction of the Diama dam is again clearly observed between the two time periods.

4.2. Regional scale analysis of groundwater chemistry

4.2.1. Contribution of multivariate statistical analysis

The SOM's technique is applied here considering 9 parameters of the available hydrochemical dataset (Table 2), which are: the electrical conductivity (CE), pH, Ca, Mg, Na, K, Cl, SO_4, and HCO_3. The matrix of components (Fig. 6) allows identifying visually the correlation between different parameters. A clear correlation is found between Na and Cl. This reflects that water mineralization is mainly controlled by these two ions. To a lesser extent, Na and Cl are correlated with Mg and SO_4. The pH is not correlated to any other element, and there is also no correlation between Ca and HCO_3, as often observed in groundwater. This will be discussed afterwards.

Similar to the analysis of piezometric variations, the application of SOM's leads to classify water samples into 4 clusters (Fig. 7). Cluster 1 is characterized by high mineralization accompanied by high levels of Na, Cl, Mg and SO_4. These groundwater samples are the most mineralized because they originate from sea water and even if they receive rainfall as water input, they

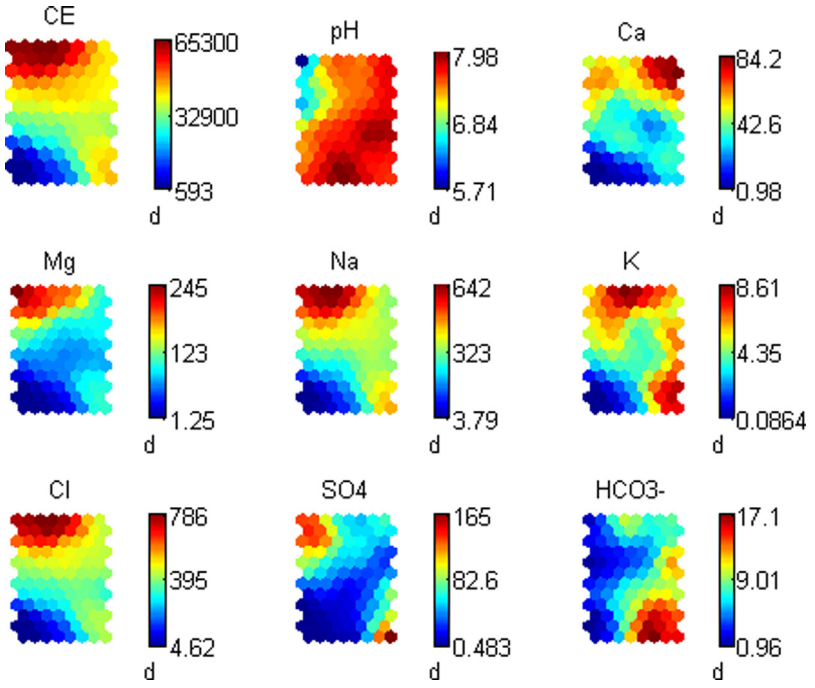

Fig. 6. Matrix of components resulting from the SOM's analysis. CE is expressed in μS/cm, chemical elements in mg/L and pH without units.

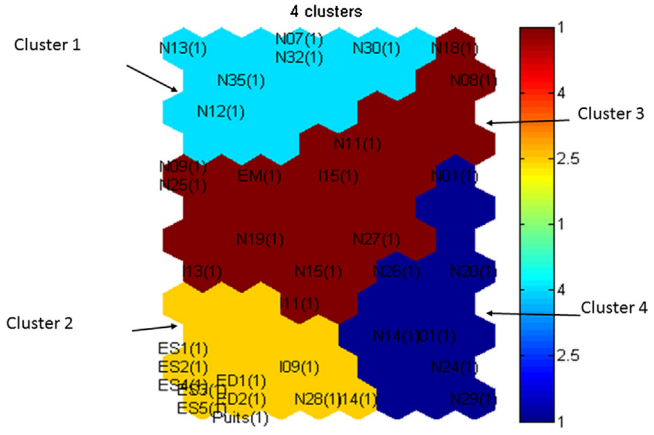

Fig. 7. Classification of water samples in four clusters with the SOM's method.

are subjected to strong evaporation. Cluster 2 is characterized by lower water mineralization. The corresponding samples come from surface water or piezometers located close to surface water streams. The lower mineralization reflects dilution by low mineralized surface water recharged from the rivers. Clusters 3 and 4 are characterized by average levels of dissolved compounds. Some of these piezometers located near surface water streams show a signature close to that of Cluster 2 while few others piezometers, located away from any influence, are similar to Cluster 1. However, most of the piezometers in Clusters 3 and 4 are located in agricultural developments. At the same time, Cluster 3 appears to be characterized by higher levels of Ca and Cluster 4 by higher levels of K and HCO_3.

The concordance between the conclusions drawn from the variations in piezometeric levels and the multivariate statistical analysis confirms that the groundwater–surface water interaction is a key driver of groundwater mineralization in the SRD.

4.2.2. Origin of groundwater salinity

Groundwater in the SRD, particularly in Group 1, shows generally a sodium chloride-facies, with a strong correlation between Na and Cl ($r = 0.94$). Representing the dataset in the Na–Cl diagram (Fig. 8) shows that points are aligned for most of them right under the sea water dilution line, with a Na/Cl ratio <0.86. Shallow groundwater in the SRB therefore corresponds to sea water which, in some places, has evaporated with time to evolve to brines (Kloppmann et al., 2011). Most groundwater samples coming from the upper part of the superficial aquifer (Nouakchottian) show a higher Na and Cl content than those coming from the lower part of the superficial aquifer (Inchirian). This indicates that evaporative processes are limited to a few meters in the subsurface.

The marine origin of groundwater in the SRD was suggested (but not demonstrated) by different former studies (Ceuppens and Wopereis, 1999; Diaw, 2008; Loyer, 1989; Ndiaye et al., 2008). It is explained by the geological history of the SRD, which was implemented during the Quaternary following successive episodes of marine transgressions and regressions. This was also amplified by frequent marine invasions that occurred on the river before the establishment of the Diama dam. The abundance of Mg, K and SO_4, ions can also be attributed to this marine origin. Indeed, these ions are abundant in seawater and they exhibit here a strong correlation (results not shown) with Na and Cl, indicating their common origin.

Na–Cl diagram can also be examined taking into consideration the 4 groups of piezometers defined previously (Fig. 8). Most of the piezometers from Group 1 are located under the sea water dilution line and they all correspond to brines. Piezometers from Group 2 are mostly located above the sea water dilution line. Some even show a net excess of sodium relative to chloride, suggesting sodium intake by cation exchange (see next section). Most of the piezometers from Group 3 and Group 4 are under the sea water dilution line. They are subject to the influence of irrigation and less mineralized than those in Group 1.

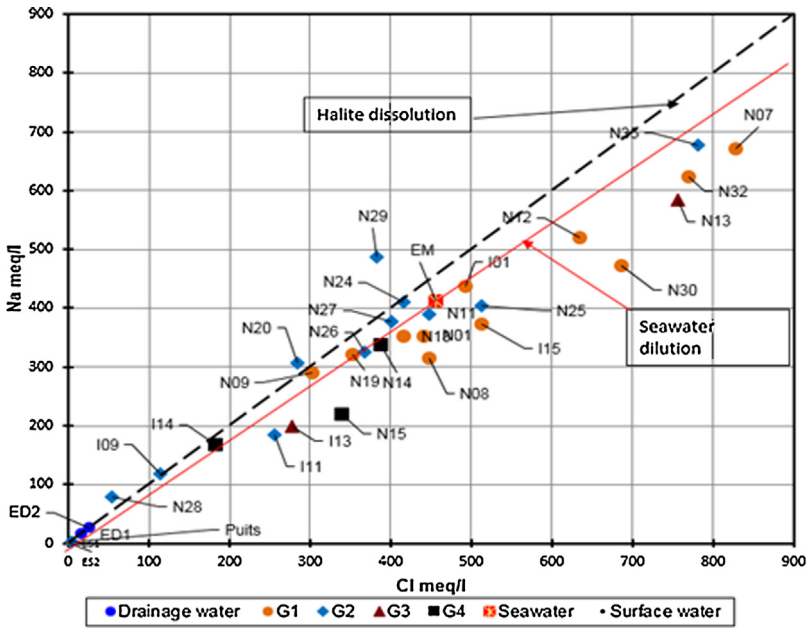

Fig. 8. Correlation diagram between Na and Cl.

4.2.3. Highlighting cation exchange processes affecting the composition of groundwater

The Piper diagram (Fig. 9a) shows that two hydrochemical facies are generally observed in the groundwater samples: calcium–bicarbonate which includes rainwater and surface water and sodium–chloride which includes, in addition to

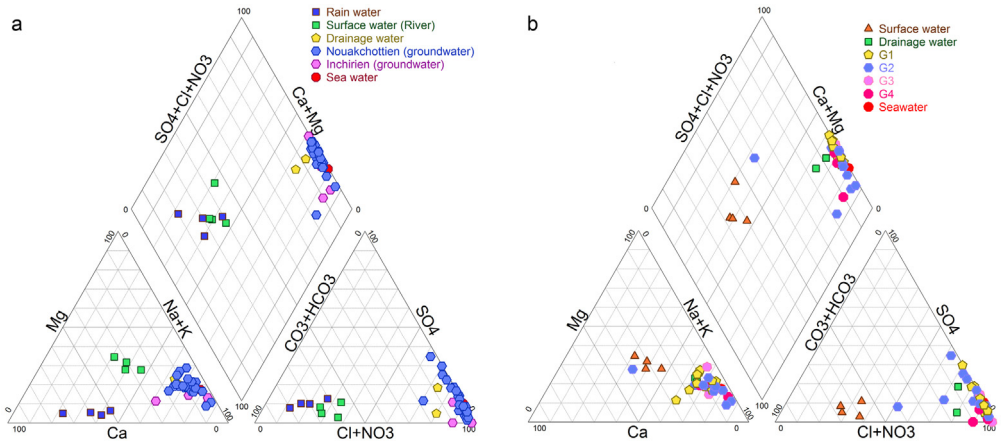

Fig. 9. Piper diagrams defining the hydrochemical facies of (a) all the samples classified in function of their origin and (b) the samples from the piezometers classified in function of the four groups defined in the previous section.

seawater, groundwater from both reservoirs and drainage water from irrigated plots. Combining the data based on the groups defined in the previous sections (Fig. 9b) allows deriving the following observations. In Group 1, most groundwater samples are enriched in calcium relative to sea water. Contrarily, in Group 2, most groundwater samples are enriched in sodium relative to calcium. In Groups 3 and 4, corresponding to irrigated plots, only piezometers located very close to rivers or irrigation canals show an enrichment in Na compared to seawater. Other piezometers show a typical sea water intrusion signature. Such changes in the chemical facies reflect Na–Ca cation exchange processes related to sea water intrusion and softening related to surface water recharge in a marine-type environment.

Fig. 10 shows the $(Ca + Mg) - (HCO_3 + SO_4)$ as a function of $(Na + K) - Cl$ where two end-members can be distinguished. The first end-member (upper left direction) corresponds to a deficit in Na + K as compared to Ca and Mg. It includes mainly piezometers of Group 1 where the aquifer is recharged by rainfall only and piezometers of Groups 3 and 4 which are under the influence of irrigation. In these sectors, groundwater is highly mineralized but depleted in sodium with respect to chloride. During the mechanism of sea water intrusion, Na was adsorbed on cation exchangers and Ca and Mg released in groundwater. In the same diagram, the second end-member shows an excess in Na with respect to Cl and to Ca and Mg deficit as compared to end-member 1. The second end-member, including samples from surface water and piezometers close to streams (Group 2), highlights chemical softening processes of formally Na-enriched waters, in relation with surface

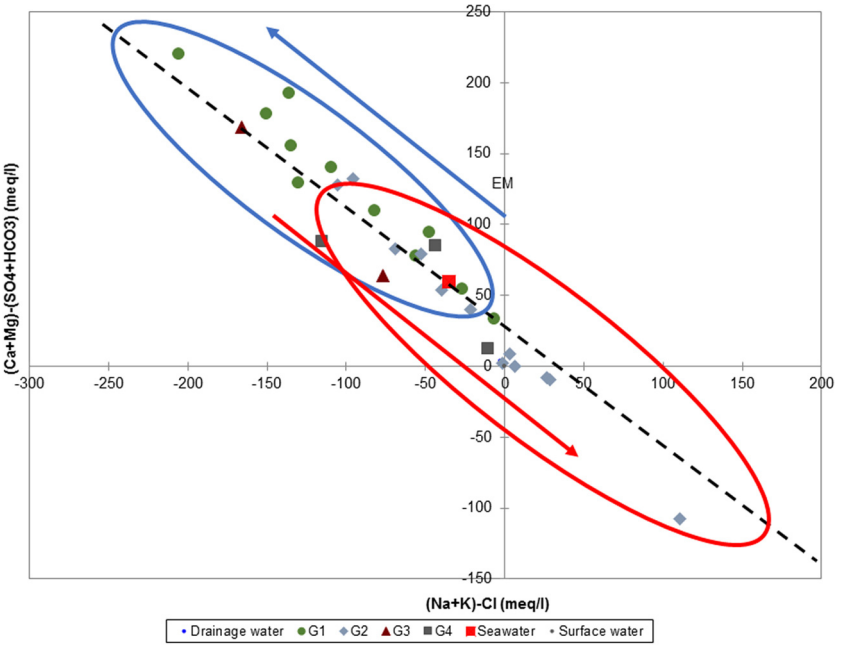

Fig. 10. $(Ca + Mg) - (HCO_3 + SO_4)$ vs $(Na + K) - Cl$.

Table 2
Results of the chemical analyses and of the calculation of saturation indices.

Sampling point	CE (µS/cm)	pH	Ca (meq/l)	Mg (meq/l)	Na (meq/l)	K (meq/l)	Cl (meq/l)	SO_4 (meq/l)	HCO_3^- (meq/l)	SI calcite	SI gypsum	SI halite
ED1	2344	7.78	3.02	5.33	14.76	0.21	17.85	1.11	3.35			
ED2	3694	7.82	4.82	7.77	24.08	0.38	27.03	6.76	2.88			
EM	41,300	7.01	20.77	92.65	413.24	6.96	455.15	52.11	2.00			
ES1	58	7.46	0.20	0.20	0.15	0.03	0.25	0.08	0.41			
ES2	83	6.98	0.24	0.25	0.27	0.03	0.22	0.04	0.53			
ES3	60	7.83	0.26	0.21	0.17	0.03	0.22	0.03	0.10			
ES4	100	7.12	0.26	0.28	0.44	0.03	0.37	0.03	0.61			
ES5	170	7.90	0.59	0.50	0.64	0.07	0.46	0.15	1.18			
I01	46,664	7.63	44.19	107.80	437.72	8.16	493.39	40.90	16.37	1.40	**−0.45**	−2.58
I09	13,092	8.13	6.90	13.91	118.91	1.77	114.37	14.73	6.40	0.93	−1.17	−3.70
I13	25,303	7.41	29.16	39.05	198.91	2.39	278.15	0.00	4.58	0.62		−3.14
I14	19,291	7.80	5.60	27.11	167.82	3.64	182.19	0.16	20.53	0.98	−3.35	−3.37
I15	46,504	7.48	167.21	69.81	373.47	2.87	512.29	41.03	3.27	1.10	**0.09**	−2.63
I11	24,438	7.72	43.27	54.17	183.93	2.20	255.39	7.11	7.56	1.27	−0.99	−3.21
N01	40,627	7.70	53.14	92.91	353.15	6.68	441.63	23.05	13.16	1.48	−0.58	−2.71
N07	68,203	7.41	37.86	194.35	670.48	7.53	828.23	41.58	12.87	0.98	−0.64	−2.16
N08	41,090	7.74	91.87	82.50	314.29	3.14	447.83	38.97	6.15	1.40	**−0.13**	−2.76
N09	33,028	6.51	44.06	119.28	289.74	6.31	302.87	128.56	1.40	−0.80	**0.05**	−2.97
N11	41,981	7.38	52.74	103.91	390.09	4.49	447.48	72.67	4.57	0.68	**−0.12**	−2.67
N12	57,970	6.84	69.99	221.25	519.52	6.19	635.10	147.40	3.67	**0.09**	**0.15**	−2.40
N13	64,802	5.11	40.83	254.64	584.40	4.92	755.25	125.51	1.06	−2.40	**−0.17**	−2.27
N14	36,400	7.59	32.42	99.29	337.44	6.73	387.66	28.09	18.38	1.31	−0.69	−2.79
N15	31,604	7.48	41.03	62.91	220.16	4.37	339.82	5.38	10.30	1.13	**−1.19**	−3.02
N18	40,350	7.75	73.37	109.68	351.82	8.03	415.62	95.51	9.93	1.48	**0.11**	−2.75
N19	34,700	7.69	36.65	72.04	321.13	4.87	352.61	50.22	3.97	0.81	**−0.34**	−2.85
N20	32,569	7.87	31.98	66.39	305.88	6.77	284.24	98.80	8.78	1.22	**−0.12**	−2.97
N24	43,231	7.65	35.71	105.91	409.66	9.51	415.84	123.13	10.09	1.08	**−0.08**	−2.69
N25	45,800	6.11	64.23	112.48	403.67	3.19	512.11	47.72	0.80	−1.25	**−0.23**	−2.60
N26	34,682	8.17	24.95	79.20	325.31	2.66	367.65	39.76	10.31	1.49	−0.61	−2.83
N27	37,978	7.67	11.65	47.62	376.30	3.91	401.67	11.90	7.68	0.63	−1.39	−2.72
N28	7510	8.11	5.45	8.33	79.57	1.01	53.77	8.85	13.29	1.20	−1.36	−4.17
N29	45,471	7.49	21.95	101.66	487.18	6.41	382.99	212.88	17.98	0.91	**−0.11**	−2.66
N30	56,480	7.32	81.94	186.94	472.71	7.35	685.54	42.42	6.36	0.91	**−0.28**	−2.40
N32	64,275	7.66	51.31	188.35	623.69	10.39	768.69	74.85	8.95	1.18	**−0.25**	−2.23
N35	64,300	7.51	66.87	226.27	678.18	7.01	780.98	157.42	3.48	0.70	**0.13**	−2.19

(Ca = calcium, Mg = magnesium, Na = sodium, K = potassium, Cl = chloride, SO_4 = sulfate, HCO_3 = bicarbonate, SI = mineral saturation index).
Calcite and gypsum saturation indexes close to zero (in the range [−0.5; 0.5] and indicative of the presence of the mineral are highlighted in bold.

water recharge. Generally speaking, this shows that recharge from surface water streams is significant, with a permanent signature on groundwater chemistry close to rivers and canals. At the same time, irrigation does not seem to have a strong influence on groundwater chemistry at the level of irrigated plots.

4.2.4. Sulfate intake by gypsum dissolution

Shallow groundwaters in the SRD are also characterized by relatively high levels of sulfate. Most samples show indeed a SO_4/Cl ratio greater than that of seawater. This suggests that another source of sulfate is active. Mineral saturation indices calculated using PHREEQc (Table 2) show that most samples are saturated with respect to gypsum which is most probably present in the sediments and constitutes an additional source of sulphate in groundwater. The presence of gypsum in the soils of the Senegal River Delta is confirmed by Deckers et al. (1996) and may even precipitate in salty soils (Ndiaye, 1999).

5. Conclusions and outlook

The SRD is a complex hydrosystem, deeply influenced by human activities, and involving several compartments, the most important being the Atlantic Ocean, surface watercourses, agricultural facilities, the depressions used for the storage of drainage water and groundwater. The analysis of the hydrodynamic and hydrochemical behavior of groundwater allows developing a conceptual model for the establishment of present hydraulic relationships and mineralization of water resources in the SRD (Fig. 11).

During former sea transgressions and flood plain submersions, sea water invaded the deltaic sediments, resulting in the occurrence of very salty groundwater in the sediments. Groundwater salinity in the shallow aquifer has been exacerbated by strong evaporative processes related to the very arid climate characterizing the SRD area, leading to the existence of brines at shallow depth of the aquifer system. In the last decades, hydrologic conditions prevailing in the SRD have evolved in relation with the rising (approx. 1.5 m) of the Senegal River stage upstream of the Diama dam and with the development of intensive irrigated agriculture in the valley. This is reflected in the hydrochemistry of groundwater close to surface water streams, with the occurrence of water softening, but not at the level of the cultivated parcels where the chemistry of groundwater does not seem to be significantly modified by the irrigation recharge, nor by natural aquifer replenishment during the rainy season.

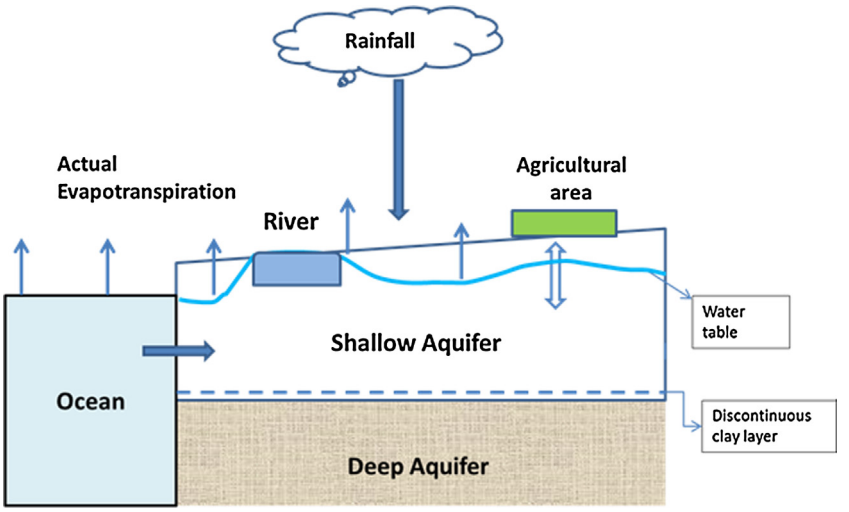

Fig. 11. Conceptual model of the hydro-system of the SRD.

The main conclusion is that the mechanism that contributes to repel salt water from the sediments corresponds to a lateral flush which has started near permanent surface water streams and not by vertical drainage and dilution with rainfall or irrigation water. If the effect of lateral flush is clearly visible, it is difficult to estimate how long it could take to come back to more favorable conditions of groundwater salinity to reduce the risks of soil salinization related to that factor. At the level of the irrigated plots, the regional hydrochemical investigation does not show any significant influence of irrigation on the evolution of the shallow groundwater. To better understand these interactions, further investigations are required at the local scale of a few irrigated parcels through a detailed assessment of water and salt dynamics between surface water and shallow groundwater.

Acknowledgement

The research project was funded by Wallonie Bruxelles International (WBI, Belgium) in the framework of the bilateral cooperation with Senegal. Field surveys were also supported by the SAED (Senegal). Chemical analyses were performed by Joel Otten from the Laboratory of Water Chemistry at the University of Liège (Belgium).

Appendix A. Supplementary data

Supplementary data associated with this article can be found, in the online version, at doi:10.1016/j.ejrh.2017.01.005.

References

Abid, K., Zouari, K., Dulinski, M., Chkir, N., Abibi, B., 2011. Hydrologic and geologic factors controlling groundwater geochemistry in the Turonian aquifer (southern Tunisia). Hydrogeol. J. 19, 415–427.
Appelo, C.A.J., Postma, D., 2005. Geochemistry, Groundwater and Pollution. CRC, Rotterdam, 649 pp., https://www.crcpress.com/Geochemistry-Groundwater-and-Pollution-Second-Edition/Appelo-Postma-Appelo-Postma/p/book/9780415364218.
Audibert, M., 1970. Delta du fleuve Sénégal: étude hydrogéologique. Projet hydro-agricole du bassin du fleuve Sénégal. Rapport projet AFR-REG-61. Généralités et rapport de synthèse: Organisation des Nations Unies pour l'alimentation et l'agriculture (FAO).
Awni, T.B., 2008. Wheathering process effects on the chemistry of the main springs of the Yarmouk Basin, North Jordan. J. Environ. Hydrol. 16 (20), 1–11.
Barbiéro, L., Laperrousaz, C., 1999. Cartographie de la salinité dans la vallée du Sénégal. In: Succès d'une démarche ascendante: Colloque GEOFCAN, Géophysique des sols et des formationssuperficielles, Orléans, France, September 20–21, 1999. BRGM, INRA, IRD, UPMC.
Barbiéro, L., Mouhamedou, A.I., Laperrousaz, C., Furian, S., Cunnac, S., 2004. Polyphasic origin of salinity in the Senegal delta and middle valley. CATENA 58, 101–124.
Belkhiri, L., Thèse de Doctorat 2011. Étude de la pollution des eaux souterraines: cas de la plaine d'Ain Azel - Est Algérien. Université Hadj Lakhdar BATNA, 175 pp.
Bourhane, A., 2010. Discrimination de l'origine de la salinité dans les eaux souterraines: (contexte hydrogéologique et méthodes d'étude). Stage de Master 2-Université de La Réunion, Sous la direction de Kloppmann W.
Ceuppens, J., Wopereis, M.C.S., 1999. Impact of non-drained irrigated rice cropping on soil salinization in the Senegal River Delta. Geoderma 92 (1–2), 125–140.
Ceuppens, J., Wopereis, M.C.S., Miézan, K.M., 1997. Soil salinization processes in rice irrigation schemes in the Senegal River Delta. Soil Sci. Soc. Am. J. 61 (4), 1122–1130.
Cogels, F.X., 1994. La qualité des eaux de surface dans le delta du fleuve Sénégal et le lac de Guiers. Mémoires de l'ORSTOM, 48 pp.
Deckers, J., Raes, D., Ceuppens, J., De Wachter, I., Merckx, R., Diallo, A., 1996. Evolution de l'acidité dans les sols du delta du fleuve Sénégal sous influence anthropogene. Etude Gest. Sols 3, 151–163.
Deutsch, W.J., 1997. Groundwater Geochemistry: Fundamentals and Applications to Contamination. Lewis Publishers, New York, 221 pp.
Diaw, E.B., (Thèse de 3ème cycle) 1996. Modélisation du transfert d'eau en milieu poreux non saturé. Application à l'étude de la recharge des nappes d'eaux souterraines en région soudano-sahélienne. Université Louis Pasteur, 304 pp.

Diaw, M., (Thèse de Doctorat de 3ème cycle) 2008. Approche hydrochimique et isotopique de la relation eau de surface/nappe et du mode de recharge dans l'estuaire et la basse vallée du fleuve Sénégal. Université Cheikh Anta Diop de Dakar, 209 pp.
Fall, S., 2006. La problématique de la gestion de l'eau à l'échelle des périmètres irrigués du Delta du fleuve Sénégal: Le bilan d'utilisation de l'eau et les coûts de l'irrigation dans les périmètres irrigués autour de l'axe hydraulique du Lampsar. Mémoire de DEA: Université Gaston Berger de Saint Louis, 97 pp.
Gac, J.Y., Carn, M., Saos, J.L., 1986. L'invasion marine dans la basse vallée du Fleuve Sénégal. Rev. Hydrobiol. Trop. 19, 3–17.
Gamble, A., Babbar-Sebens, M., 2012. On the use of multivariate statistical methods for combining in-stream monitoring data and spatial analysis to characterize water quality conditions in the White River Basin, Indiana, USA. Environ. Monit. Assess. 184, 845–875, http://dx.doi.org/10.1007/s10661-011-2005-y.
Garcia, L.A., Shigidi, A., 2006. Using neural networks for parameter estimation in ground water. J. Hydrol. 318, 215–231.
Gning, A.A., Orban, P., Ngom, F.D., Malou, R., Brouyère, S., 2012. Relation entre eaux agricoles et eaux souterraines: impact de l'irrigation sur la nappe alluviale du Delta du fleuve Sénégal. In: Colloque panafricain COPED/ANSTS, Dakar, October 30–November 3, 2012.
Gning, A.A., (PhD thesis) 2015. Etude et Modélisation Hydrogéologique des Interactions Eaux de Surface-Eaux Souterraines dans un Contexte d'Agriculture Irriguée dans le Delta du Fleuve Sénégal (Study and hydrogeological modelling of groundwater–surface water interactions in a context of irrigated agriculture in the Senegal River Delta). University of Liège and University Cheikh Anta Diop, 241 pp.
Güler, C., Thyne, G., McCray, J.E., 2002. Evaluation of graphical and multivariate statistical methods for classification of water chemistry data. Hydrogeol. J. 10 (4), 455–474.
Hong, Y.-S., Rosen, M.R., 2001. Intelligent characterisation and diagnosis of the groundwater quality in an urban fractured-rock aquifer using an artificial neural network. Urban Water 3, 193–204.
Kloppmann, W., Bourhane, A., Asfirane, F., 2011. Méthodologie de diagnostic de l'origine de la salinité des masses d'eau. Emploi des outils géochimiques, isotopiques et geéophysiques. BRGM.
Kohonen, T., 2001. Self-Organizing Maps. Springer Series in Information Sciences, vol. 30., http://dx.doi.org/10.1007/978-3-642-56927-2.
Loyer, J.Y., 1989. Les sols salés de la basse vallée du fleuve Sénégal: caractérisation, distribution et évolution sous cultures. ORSTOM, Paris, 126 pp.
Madioune, D.H., (Thèse de Doctorat en Sciences de l'Ingénieur) 2012. Etude hydrogéologique du système aquifère du horst de Diass en condition d'exploitation intensive (bassin sédimentaire sénégalais): apport des techniques de télédétection, modélisation, géochimie et isotopie. Université de Liège (ULG).
Magaritz, M., Nadler, A., Koyumdjiski, H., Dan, J., 1981. The use of Na/Cl ratios to trace solute sources in a semiarid zone. Water Resour. Res. 17 (3), 602–608.
Malou, R., (Thèse de Doctorat es Sciences) 2004. Impact du climat sur les ressources en eau souterraine en zone soudano-sahélienne. Université Cheikh Anta Diop de Dakar, 152 pp.
Michel, P., 1973. Les bassins des fleuves Sénégal et Gambie. Etude géomorphologique. ORSTOM, n° 63.
Mudry, J., 1991. Discriminant analysis an efficient means for the validation of geohydrological hypothesis. Rev. Sci. Eau 4, 19–37.
Ndiaye, B., Molénat, J., Ndoye, S., Boivin, P., Cheverry, C., Gascuel-Odoux, C., 2008. Modelling water and salt transfer in rice plantations in the Senegal river delta. Rev. Sci. Eau 21 (3), 325–336.
Ndiaye, J.P., 1999. Utilisation du phosphogypse dans les sols de la vallée alluviale du fleuve Sénégal. Institut Sénégalais de Recherche Agricole.
OMVS/USAID, 1990. Rapport de Synthèse hydrogéologique du delta du fleuve Sénégal. Projet OMVS/USAID 625-0958. Eaux souteraines; Rapport final.
Parkhurst, D.L., 1995. User's guide to PHREEQC – a computer program for speciation, reaction-path, advective-transport, and inverse geochemical calculations. U.S. Geological Survey Water-Resources Investigations Report 95-4227, 143 pp.
Peeters, L., Baçao, F., Lobo, V., Dassargues, A., 2007. Exploratory data analysis and clustering of multivariate spatial hydrogeological data by means of GEO3DSOM, a variant of Kohonen's Self-Organizing Map. Hydrol. Earth Syst. Sci. 11, 1309–1321, http://dx.doi.org/10.5194/hess-11-1309-2007.
PGE, 1998. Suivi des piézomètres dans le Delta du Fleuve Sénégal. SAED/DPDR.
Piper, A.M., 1953. A Graphic Procedure in the Geochemical Interpretation of Water Analysis, vol. 12. United States Geological Survey Groundwater Note, Washington, DC, 14 pp.
Roger, J., Serrano, O., Barusseau, J.P., Duvail, C., Noël, B.J., 2009. Notice explicative des cartes géologiques à 1/200 000 du Bassin sédimentaire sénégalais. Neuvième FED, Programme d'Appui au Secteur Minier, Projet de Cartographie du bassin sédimentaire DMG.
Sarr, R., Dabo, B., Diagne, E., Sagna, R., 2008. Terminologie et Nomenclature stratigraphique du socle et du bassin sédimentaire sénégalais. Rapport Projet PASMI 0 ACP SE 009. Infrastructures géologiques. Cartographie.
Simler, R., 2009. DIAGRAMMES: Logiciel d'hydrochimie multilangage en distribution libre. Laboratoire d'Hydrogéologie d'Avignon, France.
Trénous, J.Y., Michel, P., 1971. Etude de la structure du Dôme de Guier (Sénégal nord-occidental). Bull. Soc. Géol. Fr. 1-2, 133–139.
Ultsh, A., Herrmann, L., 2005. The architecture of emergent self-organizing maps to reduce projection errors. In: ESSANN2005 13th Eur. Symp. Artif. Neural Networks, Bruges, Belgium, pp. 1–6.
Vesanto, J., Himberg, J., Alhoniemi, E., Pearhankangas, J., 1999. Self-organizing map in Matlab: the SOM Toolbox. In: Proceedings of the Matlab DSP Conference, Espoo, Finland, November 16–17, 1999, pp. 35–40.